Journal of Organometallic Chemistry 890 (2019) 21–31

Contents lists available at ScienceDirect

Journal of Organometallic Chemistry

journal homepage: www.elsevier.com/locate/jorganchem

Different properties of P,C-donor Pd(II) and Pt(II); spectroscopic and X-ray analysis, catalytic potential and anti-proliferative potency

Abed Yousefi [a], Seyyed Javad Sabounchei [a, *], Seyed Hamed Moazzami Farida [b], Roya Karamian [b], Nosrat Rahmani [c], Robert W. Gable [d]

[a] Faculty of Chemistry, Bu-Ali Sina University, Hamedan, 65174, Iran
[b] Department of Biology, Faculty of Science, Bu-Ali Sina University, Hamedan, Iran
[c] Department of Biology, Faculty of Science, Shahed University, Tehran, Iran
[d] School of Chemistry, University of Melbourne, Victoria, 3010, Australia

ARTICLE INFO

Article history:
Received 1 February 2019
Received in revised form
27 February 2019
Accepted 2 March 2019
Available online 30 March 2019

Keywords:
Pallada-and platinaphosphacycle complexes
Phosphonium ylide
Crystallography
Mizoroki–Heck and Suzuki-Miyaura cross-coupling reactions
Antitumor activity

ABSTRACT

This account describes our recent studies on pallada-and platinaphosphacycle complexes with an unsymmetrical phosphonium ylide, $Ph_2PC(CH_2)PPh_2=C(H)C(O)C_6H_4$-*p*-$NO_2$ (**Y**), derived from 1,1-bis(diphenylphosphino)ethylene (dppee). These complexes have been prepared through reactions between (**Y**) and [MCl_2(cod)] (M = Pd (**C1**) or Pt (**C2**); cod = 1,5-cyclooctadiene) in equimolar ratio in the hope of finding new compounds that may be useful in stereoselective catalysis and find use as antitumor metallodrugs. Characterization of these compounds was performed by elemental analysis, IR, ^{1}H, ^{13}C, and ^{31}P NMR spectroscopic methods. The structures of the Pd and Pt complexes were determined by single crystal x-ray structural analyses, showing that both complexes consist of five-membered rings formed by coordination of the phosphorus ylide (**Y**) through the phosphine group and the ylidic carbon atom to the metal center. The catalytic activity of the complexes, using the Mizoroki–Heck and Suzuki-Miyaura cross-coupling reactions, have been evaluated and compared. Moreover, both compounds have been found to have antitumor activity against AGS (gastric carcinoma), MCF-7 (breast carcinoma) and A549 (non-small lung carcinoma) cells with the average of IC_{50} values from 61.19 to 290.17 μM. Generally, **C2** reveals high anticancer activity than **C1**.

1. Introduction

Phosphorus ligands are one of the most diverse and important class of ligands in chemistry [1]. Diphenylphosphines form a significant group within the large family of phosphine ligands which includes ligands such as 1,1-bis(diphenylphosphino)methane (dppm), 1,2-bis(diphenylphosphino)ethane (dppe) and many others that play a key role in the synthesis of transition metal complexes and have broad applications in industrial, biological and chemical synthesis [2,3]. Biphosphorus ylides can coordinate to metal ions in three modes as displayed in Chart 1: monodentate (P-coordinated [4], C-coordinated [5] or O-coordinated [6]), bidentate (or chelating) [3] and bridging modes [7] (chart 1).

One of the diphenylphosphine analogs is 1,1-bis(diphenylphosphino)ethylene (dppee), a ligand that has extremely low-lying π* orbitals, mainly located around the sp^2-hybridized phosphorus atoms, that have a marked tendency to engage in metal to phosphorus π-back bonding. This property is useful for catalysis, leading to highly efficient organic transformations with a diverse range of selectivity. Complexes derived from the IB and IIB groups (platinum, palladium, rhodium and ruthenium), in particular, have shown a wide range of catalytic, biological and industrial properties, among others [8–11]. Compared to other transition metal complexes, from the catalytic point of view, palladium-based organometallic compounds are the most reactive in a number of different coupling reactions, in particular their 0, I, II and IV oxidation states [12,13]. Due to the importance of palladium-catalysis in scientific and industrial chemistry, a number of publications and reviews describing various aspects of this topic have recently been published [14]. The

* Corresponding author.
E-mail address: jsabounchei@yahoo.co.uk (S.J. Sabounchei).

https://doi.org/10.1016/j.jorganchem.2019.03.002
0022-328X/

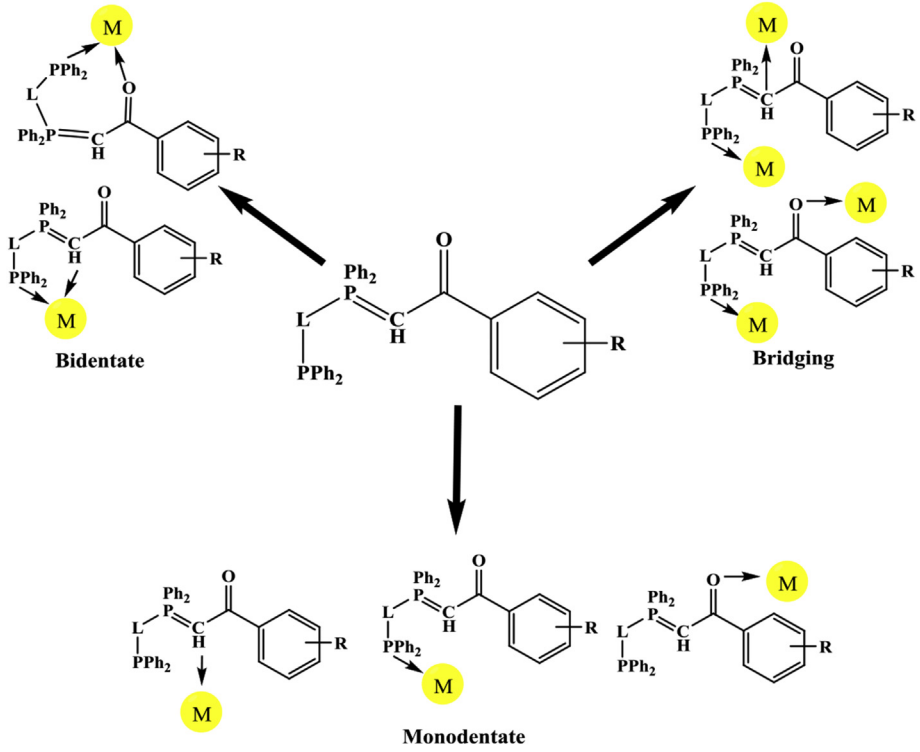

Chart 1. Possible binding modes of phosphorus ylides to the metal M.

investigation of the reactivity and coordination chemistry of metal complexes (Pd, Pt and Rh, especially) derived from various ylides has been an important research focus of our group [2,15,16]. This article presents the significant catalytic application of new complexes with new a phosphorus ligand containing a metallated sp^3-carbon center ("pallada-and platinacycles") with a C-P chelate coordination. We have also shown that phosphorus analogs have significant biological properties, such as antioxidant and antibacterial activity [17]. Many cancers, such as lung, breast and gastric cancer, are still difficult to treat and are a source of serious health problems in many countries, and every year cause many deaths worldwide [18]. Accordingly, researchers have attempted to produce compounds with high anticancer potential. Among the drugs already discovered, inorganic compounds have a special role in this field [19,20], in particular platinum and its derivatives, which are important chemotherapy drugs used to treat various cancers [21]. After the discovery of the anticancer activity of cis-diamineplatinum(II) dichloride (cisplatin) [22], a variety of inorganic anticancer drugs, such ascarboplatin [23] andoxaliplatin [24], are being routinely used as a part of cancer treatment in patients. Although the platinum-based drugs have been used for about four decades, several side effects, such as nephrotoxicity and drug resistance of the tumor cells, have raised real challenges to researchers. In order to decrease these side effects, researchers have been prompted to look for alternatives to inhibit or kill tumor cell growth [25,26]. There seems to be a number of properties that could explain the anti-proliferative activity of the Pt complexes. In addition to the nature of platinum metal, the structure of the complex and the type of the ligands, are some of the important properties. In the present study, our goal is to expand the scope of these complexes to new pallada-and platinaphosphacycle complexes having both phosphorus and carbon donor atoms and comparing their intriguing functionalities including anti-proliferative potency and catalytic activities. Furthermore, we report *in vitro* testing of the preliminary anticancer activity on the human AGS gastric, MCF-7 breast and A-549 lung cancer cell lines.

2. Experimental

2.1. Materials and methods

Phosphorus ylide $Ph_2PC(CH_2)_2PPh_2C(H)C(O)C_6H_4$-*p*-$NO_2$ (Y) was prepared according to literature methods [27]. Synthesis of Pd/Pt(II) complexes was carried out with dry solvents and under a nitrogen atmosphere using standard Schlenk techniques. $[MCl_2(cod)]$ (M = Pd or Pt) complexes were prepared according to previously published procedures [28]. Dichloromethane was used as reagent grade and dried over P_2O_5. Elemental analysis was performed on a Leco, CHN-932 apparatus. The ^1H, ^{13}C and ^{31}P NMR spectra were recorded on BrukerAdvance 250 MHz and Jeol 90 MHz spectrometers in $CDCl_3$ or DMSO-d_6 as solvents at 25 °C. IR spectra were recorded on KBr pellets using a Shimadzu 435-U04 spectrophotometer in the region of 4000–400 cm^{-1}.

2.2. Synthesis of data salt [$(Ph_2PC(CH_2)PPh_2CH_2C(O)C_6H_4$-p-$NO_2$] Br(S)

An acetone solution (10 ml) of ketone (1 mmol) was added to an acetone solution (10 ml) of dppee (1 mmol). The mixture was stirred under nitrogen atmosphere for 15 h. The resulting white solid was filtered off and dried. Yield: 91%, M.p: 201–203. *Anal.* Calc. for $C_{34}H_{28}O_3NP_2Br$ (%): C, 63.76; H, 4.41; N, 2.19. Found: C, 63.84; H, 4.52, N, 2.27. Selected IR absorption in KBr (cm^{-1}): 1682 (CO). ^1H NMR (89.6 MHz, $CDCl_3$) δ_H (ppm): 6.21 (d, CH_2, 2H, $^2J_{P-H} = 12.54$ Hz); 6.96 (br, CH_2, 2H merged with aromatics); 7.53–8.48 (m, 24H, Ar). ^{31}P NMR (36.26 MHz, $CDCl_3$) δ_P (ppm): −15.26 (d, PPh_2, $^2J_{P-P} = 102.25$ Hz), 20.50 (d, PCH, $^2J_{P-P} = 102.25$ Hz). ^{13}C NMR (62.89 MHz, $CDCl_3$) δ_C (ppm): 38.63 (d,

CH_2); 116.27–150.98 (Ar and CH_2); 191.24 (s, CO).

2.3. Synthesis of data ylide ($Ph_2PC(CH_2)PPh_2CHC(O)C_6H_4$-p-$NO_2$(Y))

0.1 ml of Et_3N was added dropwise to 10 mL toluene solution included 1 mmol of salt **(S)**. After 2 h the mixture was filtered and petroleum benzene was added to the filtrate to give a yellow powder. Yield: 45%, M.p: 149–152. *Anal*. Calc. for $C_{34}H_{27}NO_3P_2$ (%): C, 72.98; H, 4.86; N, 2.51. Found: C, 73.09; H, 4.96; N, 2.59. Selected IR absorption in KBr (cm^{-1}): 1588 (CO). ^{1}H NMR (89.6 MHz, $CDCl_3$) δ_H (ppm): 4.27 (d, CH, 1H). 6.76 (br, CH_2, 2H merged with aromatics); 7.17–8.18 (m, 24H, Ar). ^{31}P NMR (36.26 MHz, CDCl3) δ_P (ppm): −14.37 (d, PPh_2, $^2J_{P-P} = 88.47$ Hz), 16.55 (d, PCH, $^2J_{P-P} = 88.47$ Hz). ^{13}C NMR (62.90 MHz, $CDCl_3$) δ_C (ppm): 52.90 (d, CH); 122.95–148.14 (Ar and CH_2); 181.77 (s, CO).

2.4. Synthesis of data Pd(II) complex $PdCl_2(Ph_2PC(CH_2)PPh_2CHC(O)C_6H_4$-p-$NO_2$ (C1)

A dichloromethane solution of 0.5 mmol of ylide **(Y)** (15 mL) was added to a 0.5 mmol dichloromethane solution (5 mL) of $PdCl_2$(cod). The mixture was stirred for 8 h under a nitrogen atmosphere. Petroleum ether was added to the solution and the resulting yellow powder was dried. Yield: 83%, M.p: 221–223. *Anal*. Calc. for $C_{34}H_{27}NO_3P_2PdCl_2$ (%): C, 55.42; H, 3.69; N, 1.91. Found: C, 55.51; H, 3.62; N, 1.84. Selected IR absorption in KBr (cm^{-1}): 1622 (CO). ^{1}H NMR (89.6 MHz, $CDCl_3$) δ_H (ppm): 5.66 (d, CH, 1H, $^2J_{P-H} = 7.16$ Hz); 6.91 (br, CH_2, 2H merged with aromatics); 7.35–8.21 (m, 24H, Ar). ^{31}P NMR (36.26 MHz, $CDCl_3$) δ_P (ppm): 32.02 (d, PPh_2, $^2J_{P-P} = 36.98$ Hz), 35.77 (d, PCH, $^2J_{P-P} = 36.98$ Hz). ^{13}C NMR (62.89 MHz, $CDCl_3$) δ_C (ppm): 33.17 (d, CH); 120.00–151.30 (Ar and CH_2); 193.82 (s, CO).

2.5. Synthesis of data Pt(II) complex $PtCl_2(Ph_2PC(CH_2)PPh_2CHC(O)C_6H_4$-p-$NO_2$ (C2)

A dichloromethane solution of 0.027g (0.05 mmol) of ylide **(Y)** (15 mL) was added to a 0.018g (0.05 mmol) dichloromethane solution of $PtCl_2$(cod) (5 mL). The mixture was stirred for 8 h under nitrogen atmosphere. Petroleum ether was then added to the solution and the resulting white powder was dried. Yield: 63%, M.p: 245–247. *Anal*. Calc. for $C_{34}H_{27}NO_3P_2PtCl_2$ (%): C, 49.47; H, 3.30; N, 1.70. Found: C, 49.55; H, 3.36; N, 1.75. Selected IR absorption in KBr (cm^{-1}): 1629 (CO). ^{1}H NMR (89.6 MHz, $CDCl_3$) δ_H (ppm): 5.60 (d, CH, 1H, $^2J_{P-H} = 12.54$ Hz); 6.65 (br, CH_2, 2H merged with aromatics); 7.25–8.14 (m, 24H, Ar). ^{31}P NMR (36.26 MHz, $CDCl_3$) δ_P (ppm): 11.99 (d, PPh_2, $^2J_{P-P} = 33.36$ Hz, $^1J_{Pt-P} = 895.62$ Hz), 32.69 (d, PCH, $^2J_{P-P} = 33.36$ Hz). ^{13}C NMR (62.89 MHz, $CDCl_3$) δ_C (ppm): 26.32 (d, CH); 128.38–150.56 (Ar and CH_2); 193.38 (s, CO).

2.6. Crystallography

Yellow crystals of **C1** and pale yellow crystals of **C2** were crystallized by vapour diffusion of diethyl ether into deuterochloroform. The crystals were long thin needles, attempts to cut them to smaller size resulted in them fracturing, or becoming too disordered to be usable. Crystals of both compounds showed evidence of disorder, however attempts to obtain better crystals were not successful. Both structures are isomorphous. Data collection for **C1** was carried out on a Rigaku Oxford Diffraction SuperNova, Dual Source (Cu at zero) Atlas diffractometer at 130 K, while data collection for **C2** was carried out on an XtaLAB Synergy, Dualflex, HyPix diffractometer at 100 K; for both crystals mirror monochromated Cu Kα radiation (λ = 1.54018 Å) was used. Gaussian absorption corrections [29] were applied to the data. Using Olex2 [30], the structures were solved with the ShelXT [31]structure solution program using Intrinsic Phasing and refined with the ShelXL [32] refinement package using Least Squares minimization on F^2, using all data. All non-hydrogen atoms were refined with anisotropic displacement parameters, while all hydrogen atoms were placed at geometrical estimates and refined using the riding model with an isotropic displacement parameter equal to 1.2 times U_{eq} of the parent atom. Both structures showed residual electron density peaks around the metal atoms due to minor disorder, 2.47 eÅ^{-3} and -1.80 eÅ^{-3} for **C1**, and 2.41 eÅ^{-3} and -2.42 eA^{-3} for **C2**; attempts to model this disorder were not successful.

2.7. Typical procedure for the catalytic coupling reactions

A vial charged with metalacycle as a catalyst (0.005 mmol), relevant reagent (olefin for Mizoroki-Heck and arylbronic acid for Suzuki-Miyaura coupling reactions) (0.75 mmol), aryl chloride (0.5 mmol), base (1.0 mmol) and solvent (2 ml) was heated to reflex temperature for 6 h in the presence of air. The reactions were monitored by thin-layer chromatography (TLC). After cooling, the mixture was extracted with n-hexane:EtOAc, filtered and purified by recrystallization (from ethanol and water) or purified by silica gel column chromatography (n-hexane:EtOAc).

Among the aryl halide reagents, couplings of aryl bromides and iodides investigations have shown that aryl iodides and bromides were more reactive than aryl chlorides [4]. The small C–I and C-Br bond dissociation energies, compared to the larger C–Cl bond dissociation energy, and easier oxidative addition to the Pd(0) species results in the aromatic iodides and bromides having a higher reactivity compared to aryl chlorides in the coupling reactions [33]. Aryl chlorides are ideal substrates for coupling reactions since they are cheaper and more widely available than their bromide or iodide analogs The challenge of activating the C–Cl bond of aryl chlorides, as well as the financial aspects, means that research is now focused on increasing the efficiency of aryl chlorides in cross-coupling reactions [34]. Accordingly, we have attempted to synthesize compounds that can increase the catalytic properties of aryl chlorides in the Mizoroki-Heck and Suzuki-Miyaura coupling reactions.

The activity of complexes **C1** and **C2** when used as catalysts in the Mizoroki-Heck and Suzuki–Miyaura coupling reactions has been determined. In order to obtain the optimum experimental conditions, we carried out a model reaction including base, solvent and catalyst loading (Tables 1 and 2).

Mizoroki-Heck coupling reaction: The reaction of styrene with chlorobenzene in DMF/H_2O (1:1) at 110 °C in the presence of K_3PO_4 (1 mmol) and 0.05 mmol of complexes **C1** and **C2** as catalyst was chosen as a model reaction, which led to related product in 61% and 18% yields for complexes **C1** and **C2** respectively. (Table 1, entry 1). Subsequently, a series of experiments were performed to find the optimum conditions. At the first stage, we studied the efficacy of base and solvent on the coupling reaction. This optimization was done with commonly used bases and solvents, including organic and inorganic bases and aqueous protic and aprotic solvents. Two parameters of base potency; solubility and basicity; depend on the solvent that is used. Thus the coupling reactions give the desired products in moderate to high yields when carried out in the presence of K_2CO_3 and K_3PO_4 (Table 1, entries 2, 5 and 1, 4). However, due to the low solubility of this organic base in aqueous solvents, the reactions in the presence of NEt_3 did not proceed efficiently even after prolonged stirring at the reflux temperature of the solvents (Table 1, entries 3 and 6). Among the tested aqueous solvents, DMF/H_2O gave higher yields of coupled product, while the reactions in water or non-aqueous DMF led to lower yields, indicating the important role of the solubility of the base in such catalytic

Table 1
Reaction conditions for Mizoroki-Heck coupling reaction.

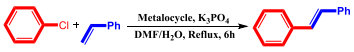

Entry	Base	Solvent	Catalyst loading(mmol)	Yield (%)
1	K_3PO_4	DMF/H_2O	0.05	61[a]/18[b]
2	K_2CO_3	DMF/H_2O	0.05	69[a]/27[b]
3	NEt_3	DMF/H_2O	0.05	51[a]/-[b]
4	K_3PO_4	$Methanol/H_2O$	0.05	38[a]/13[b]
5	K_2CO_3	$Methanol/H_2O$	0.05	46[a]/24[b]
6	NEt_3	$Methanol/H_2O$	0.05	20[a]/-[b]
7	K_2CO_3	H_2O	0.05	43[a]/-[b]
8	K_2CO_3	DMF	0.05	51[a]/18[b]
9	K_2CO_3	Methanol	0.05	69[a]/-[b]
10	K_2CO_3	DMF/H_2O	0.005	51[a]/-[b]
11	K_2CO_3	DMF/H_2O	0.1	71[a]/30[b]

[a] *Yielded for complex **C1**.*
[b] *Yielded for complex **C2**.*

Table 2
Reaction conditions for Suzuki–Miyaura coupling reaction.

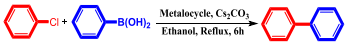

Entry	Base	Solvent	Catalyst loading(mmol)	Yield (%)
1	Cs_2CO_3	Ethanol	0.05	73[a]/34[b]
2	K_2CO_3	Ethanol	0.05	71[a]/21[b]
3	NEt_3	Ethanol	0.05	49[a]/-[b]
4	NaOAc	Ethanol	0.05	51[a]/-[b]
5	Cs_2CO_3	Hexane	0.05	34[a]/21[b]
6	Cs_2CO_3	NMP	0.05	58[a]/28[b]
7	Cs_2CO_3	H_2O	0.05	39[a]/21[b]
8	Cs_2CO_3	Toluene	0.05	26[a]/-[b]
9	Cs_2CO_3	Ethanol	0.005	69[a]/-[b]
10	Cs_2CO_3	Ethanol	0.1	78[a]/41[b]
11	Cs_2CO_3	Ethanol	0.05	73[a]/34[b]

[a] Yielded for complex **C1**.
[b] Yielded for complex **C2**.

systems (Table 1, entries 2, 7 and 8).

Suzuki–Miyaura coupling reaction: the catalytic performance of the complexes **C1** and **C2** in the Suzuki–Miyaura cross-coupling reaction also was examined. The reaction of phenylboronic acid with chlorobenzene in ethanol (1:1) at reflux temperature in the presence of Cs_2CO_3 (1 mmol) and 0.05 mmol of complexes **C1** or **C2** as catalyst was chosen as a model reaction, which provided the coupled product in 73% yield for complex **C1** and 34% for **C2**(Table 2, entry 1). The solvent optimization stage was done with several common solvents and using ethanol as a solvent gave the highest yield for this reaction. The reactions using water, however, required additional time for completing the coupling reaction (Table 2, entry 7). As well, non-polar solvents such as hexane and toluene gave low conversions (Table 2 entries 5 and 8). After that, we optimized the base from those commonly used. As mentioned above, base plays an important role in such cross-coupling reactions and has a striking accelerating effect on the reaction time. Among the tested bases, Cs_2CO_3 and K_2CO_3, were the most effective base for the reactions (Table 2, entries 1 and 2), while other bases, such as NEt_3 (as an organic base) or NaOAc, proved to be less active (Table 2, entries 3 and 4). According to the optimized reaction conditions (EtOH, Cs_2CO_3 and 0.005 mmol of catalyst) various types of functionalized aryl halides reacted with arylboronic acid and were converted into the corresponding coupled products in high to excellent yields.

2.8. Cytotoxic studies

2.8.1. Cell culture

As malignant cells, the human breast (MCF-7; IBRC C10082), lung (A549; IBRC C10080) and gastric (AGS; IBRC C10071) adenocarcinoma cell lines were purchased from Iranian Biological Resource Center (IBRC; Tehran, Iran). Breast and lung cell lines were cultured in DMEM:Ham's F12 supplemented with 10% Fetal Bovine Serum (FBS), 100 units ml^{-1} penicillin, 100 μg ml^{-1} streptomycin, and L-glutamine. AGS cell line was also grown in Ham's F12 medium supplemented with the same materials. Cells were maintained at 37 °C in a humidified atmosphere with 5% CO_2 in the air.

2.8.2. Solutions

Both compounds were dissolved in DMSO at a concentration of 20 mmol l^{-1} as a stock solution and diluted in culture medium at concentrations of 1.56, 3.13, 6.25, 12.50, 25 and 50 mmol l^{-1} as working solution. To evade DMSO toxicity, the concentration of DMSO was less than 0.5% (v/v) in all experiments.

2.8.3. Cell viability assay

The assay was performed according to a modified cell viability (MTT) method. This assay detects the reduction of MTT (3-[4,5-dimethylthiazolyl]-2,5-diphenyltetrazolium bromide) by mitochondrial dehydrogenase, to blue formazan product, which reflects the normal functioning of mitochondrial and cell viability [35].

Briefly, the cells (5×10^4) were equally divided in each well containing 100 μL of the RPMI medium supplemented with 10% FBS in a 96-well plate. After 24 h for adhesion, a serial of doubling dilution of the compounds was added to triplicate wells over the range of 0–50 μM. The final concentration of DMSO in the culture medium was maintained at 0.5% (v/v) to avoid toxicity of the solvent [36]. After 12 h, 10 μl of MTT (5 mg ml^{-1} stock solution) was added and the plates were incubated for an additional 4 h at 37 °C. The medium was discarded and the formazan blue, which formed in the cells, was dissolved with 100 μl DMSO. The optical density (OD) values of each well were measured by using ELISA plate reader (infinite F50, TECAN, Austria) at 490 nm wavelength. The cell survival curves were calculated from cells incubated in the presence of 0.5% DMSO. Cytotoxicity is expressed as the concentration of the compounds inhibiting cell growth by 50% (IC_{50}), ($y = 16.788x + 26.55$; $r^2 = 0.968$). All tests and analyses were run in triplicate and mean values recorded.

2.8.4. Statistical analysis

The results were analyzed by Analysis of Variance (ANOVA) and Duncan test. The data were expressed as mean value for 3 independent assays ±S.D. All significance tests were set at $P \leq 0.05$, and the statistics were analyzed using the SPSS software (IBM Corp. Released in 2013. IBM SPSS Statistics for Windows, Version 22.0. Armonk, NY: IBM Corp.) with the level of significant difference between compared data sets being set at $P < 0.05$.

3. Results and discussion

3.1. Spectroscopy

Based on various reports in literature, it can be concluded that the ylidic compounds are a subclass of zwitterions. According to the Scheme 1, the ylidic form of **Y** without formal charges can be represented as a zwitterionic form, which contains simultaneously one positive phosphine and one negative carbonyl group. The molecule as a whole is electrically neutral and the reaction of this bifunctionaldiphosphine-based dipolar ligand with either [MCl_2(cod)] (M = Pd and Pt; cod = 1,5-cyclooctadiene) led to the P,C-chelated palladium(II) and platinum(II) complexes **C1** and **C2**, respectively, without any evidence of by-product formation.

The spectroscopic methods used in the present study include ^1H, ^{13}C and ^{31}P NMR and other conventional techniques such as IR and elemental analysis. A brief summary of these data is shown in Table 3. As well, the structures of the complexes **C1** and **C2** were determined by single crystal X-ray structural analyses that confirming a 1:1 stoichiometry between the MCl_2 (M = Pd or Pt) and the phosphorus ylide in the complexes.

In the chelating coordination mode through the carbon atom there should be an increase in the υ(CO) frequency, while for O-coordination a lower shift for this frequency in the IR region is expected [37]. The υ(CO) occurs at 1588 cm^{-1} in the parent ylide **Y,** while this absorption band of the complexes shows a significant shift to 1625 cm^{-1}, compared with its phosphorus ylide **Y.** This is a consequence of resonance removing between P^+-C^- and carbonyl group in **Y**. The resonance between the zwitterionic and ylidic forms of **Y** decrease the bond order of the carbonyl group and lead to lower C=O stretching frequency. However, the resonance was disturbed in complexes (Scheme 1) and accordingly, we see a shift to higher frequency in complexes compared to **Y** [38]. Overally, these results are consistent with the chelation occurs through the ylidic carbon atom and free PPh_2 group of the ylide to Pd(II) and Pt(II) chlorides [7,27].

Likewise, in the ^1H NMR spectra, chemical shifts show all the expected resonances of these complexes respect to the ylide **Y** (see Supplementary data). The values for both complexes appear to be shifted downfield compared to the parent ylide, as a consequence of the P,C-coordination character of the ylide [3,16,27,39].

The ^{31}P chemical shift values for the complexes also appear to be shifted downfield respect to the parent ylide, indicating that coordination of the ylide has occurred (Fig. 1). Complexes **C1** and **C2** have two unequal phosphorus groups, PPh_2 and $P(Ph_2)CH$. As expected, the ^{31}P NMR spectrum of **C1** exhibits two doublets around 32 and 36 ppm attributed to the PPh_2 and $P(Ph_2)CH$ phosphorous atoms, respectively (Fig. 1). The ^{31}P NMR spectrum of **C2** is more complex, showing peaks with downfield shifts at around 10 and 33 ppm along with two satellite peaks, around −7 and 31 ppm, due to ^{195}Pt–^{31}P coupling with the adjacent PPh_2 phosphorous, one of these peaks has almost merged with a peak due to the $P(Ph_2)CH$ phosphorous atom. It must be noted that O-coordination of the ylides generally leads to the formation of cis and trans isomers, giving rise to two different signals in the ^1H and ^{31}P NMR spectra [40].

The most important aspect of ^{13}C NMR spectra of these complexes is the downfield shift of the carbonyl group signals, around 193 ppm, compared to the same carbon in the parent free ylide, 181 ppm, indicating a much lower shielding of the carbon of the CO group in these complexes (see Supplementary data). The change in hybridization of the ylidic carbon in complexes respects to ylide leads to mentioned downfield shift that has been previously observed in the series of Pd(II) and Pt (II) complexes [41]. Thus, the spectral data clearly indicates the bidentate coordination of the ylides through both the phosphine group and the ylidic carbon atom.

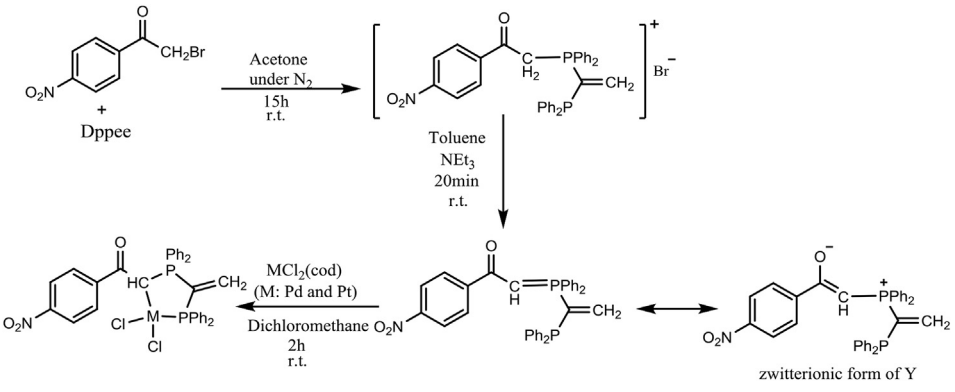

Scheme 1. Synthesis of compounds S, Y, C1 and C2.

Table 3
Selected spectroscopic data for compounds.

Compound	IR; ν(CO) cm^{-1}	^{31}PNMR; δ(PCH) and δ(PPh_2) ppm	^{1}H NMR; δ(PCH) ppm	^{13}C NMR; δ(CO) ppm
Salt **(S)**	1682	−15.26, 20.50	6.21	191.24
Ylide **(Y)**	1588	−14.37, 16.55	4.27	181.77
[P, C→Pd] **(C1)**	1622	32.02, 35.77	5.66	193.83
[P, C→Pt**] (C2)**	1629	11.99, 32.69	5.60	193.38

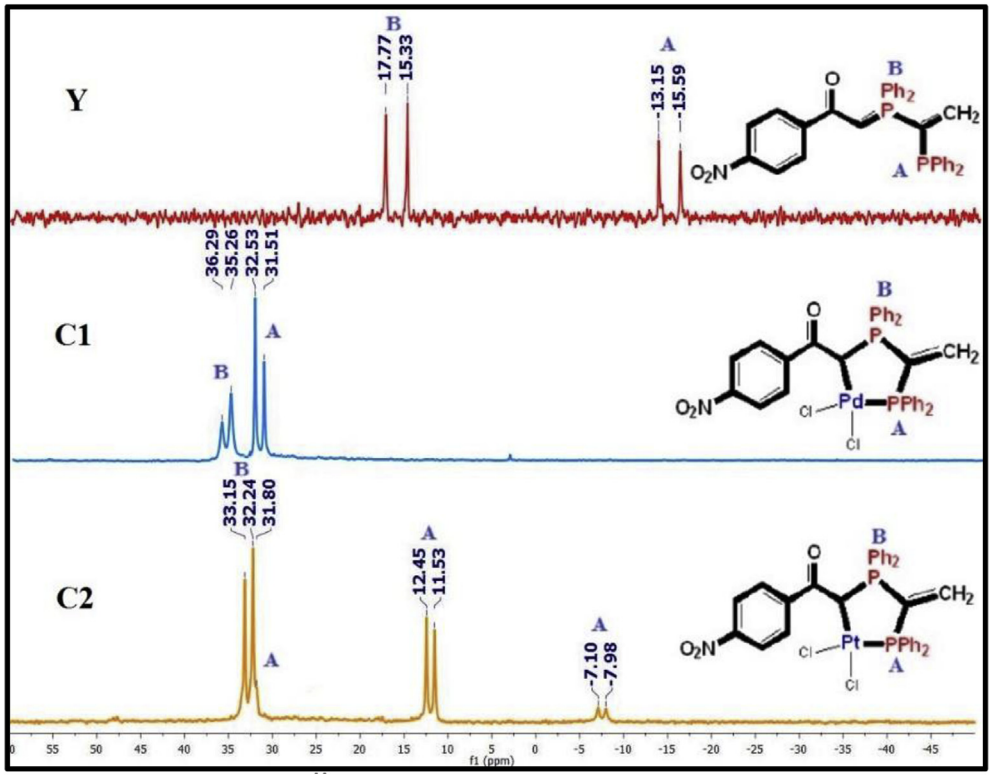

Fig. 1. ^{31}P NMR spectra of Y (a), C1 (b) and C2 (c).

3.2. X-ray data collection and structure determination

Crystals, suitable for single-crystal X-ray analysis, of complexes **C1** and **C2** were grown by vapour diffusion of diethyl ether into a $CDCl_3$ solution. The molecular structures of these complexes are shown in Figs. 2 and 3. Crystal data are given in Table 4, while selected bond distances and angles for the two structures, **C1** and **C2,** are presented in Table 5.

C1 and **C2** are isostructural, with only minor differences in bond lengths and angles. The structure of C1 is described, with

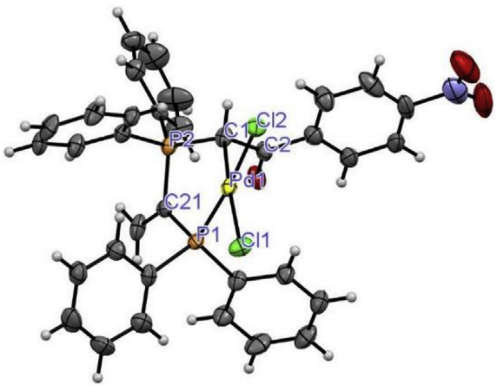

Fig. 2. ORTEP view of X-ray crystal C1.

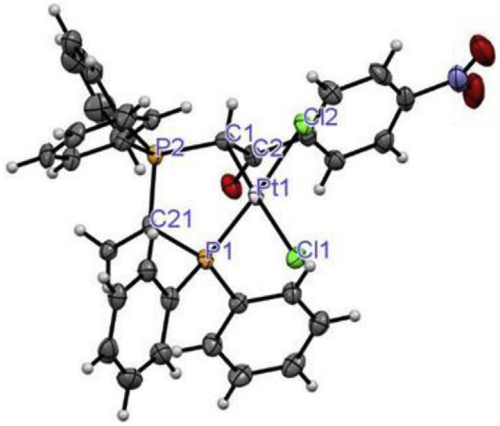

Fig. 3. ORTEP view of X-ray crystal C2

Table 4
Data collection and refinement statistics for C1 and C2.

	C1	C2
Empirical formula	$C_{34}H_{27}Cl_2NO_3P_2Pd$	$C_{34}H_{27}Cl_2NO_3P_2Pt$
Formula weight	736.80	825.49
Crystal system	orthorhombic	orthorhombic
Space group	Pbca	Pbca
a/Å	18.8710(5)	18.9685(2)
b/Å	15.6752(3)	15.71890(16)
c/Å	21.0265(5)	20.8678(3)
α/°	90	90
β/°	90	90
γ/°	90	90
Volume/Å^3	6219.8(3)	6222.01(12)
Z	8	8
ρ_{calc}g/cm^3	1.574	1.762
μ/mm^{-1}	7.666	11.289
F(000)	2976.0	3232.0
Crystal size/mm^3	0.511 × 0.1 × 0.021	0.536 × 0.107 × 0.01
2Θ range for data collection/°	8.41 to 133.182	8.446 to 133.202
Reflections collected	40481	53272
Independent reflections	5498	5502
Data/restraints/parameters	5498/0/388	5502/0/388
Final R indexes [I ≥ 2σ (I)]	$R_1 = 0.0808$, $wR_2 = 0.2067$	$R_1 = 0.0397$, $wR_2 = 0.0959$
Final R indexes [all data]	$R_1 = 0.0966$, $wR_2 = 0.2202$	$R_1 = 0.0455$, $wR_2 = 0.1004$
Largest diff. peak/hole/e Å^{-3}	2.47/-1.80	2.41/-2.42

Table 5
Selected bond lengths [Å] and bond angles [°] for C1 and C2

C1		C2	
Bond distances			
Pd1-Cl1	2.343(2)	Pt1-Cl1	2.3545(13)
Pd1-Cl2	2.376(2)	Pt1-Cl2	2.3713(12)
Pd1-P1	2.231(2)s	Pt1-P1	2.2096(13)
Pd1-C1	2.117(8)	Pt1-C1	2.085(5)
P1-C21	1.855(8)	P1-C21	1.842(5)
P1-C23	1.818(9)	P2-C21	1.809(6)
O1-C2	1.233(11)	O1-C2	1.233(7)
Bond angles			
Cl1-Pd1-Cl2	92.80(8)	Cl1-Pt1-Cl2	90.66(4)
P1-Pd1-Cl1	88.03(8)	P1-Pt1-Cl1	90.13(5)
P1-Pd1-Cl2	174.01(8)	P1-Pt1-Cl2	174.64(5)
C1-Pd1-Cl1	173.6(2)	C1-Pt1-Cl1	175.48(15)
C1-Pd1-Cl2	90.3(2)	C1-Pt1-Cl2	89.16(15)
C1-Pd1-P1	89.5(2)	C1-Pt1-P1	90.47(15)
P2-C21-P1	109.1(4)	P2-C21-P1	109.2(3)

corresponding details for C2 in brackets. The Pd atom in **C1** and the Pt atom in **C2** are both in a slightly distorted square planar environment, coordinated by one phosphorous and one carbon atom, from the chelating ylide, and by two cis-coordinating chlorides; the four coordinating atoms show a slight tetrahedral distortion with a rms deviation of 0.115 Å (0.096 Å) and with the Pd atom lying almost in the plane, the deviation being 0.005(2)Å (0.0098(15) Å). The five-membered ring comprising Pd1, P1, P2 C21 and C1 is in an envelope conformation, with C1 lying 0.820(8) Å (0.824(5) Å) out of the plane of the other four atoms. The Pd-Cl distance trans to the ylidic carbon atom, 2.343(2) Å (2.3545(13)), is slightly shorter than the corresponding distance trans to the phosphorous atom, 2.376(2)Å (2.3713(12)). The dihedral angle between the keto group and the attached aromatic ring is 12.5(5)° (14.0(3)°), while the dihedral angle between this aromatic ring and the nitro group is 18.6(15)° (18.5(8)°). For both structures weak C-H…O, C-H…Cl hydrogen bonds, π … π, C-H … π and NO … π interactions link the molecules into a 3D network.

3.2.1. Catalytic coupling reaction

Several mechanistic pathways, depending on the nature of the catalyst, have been investigated for the Heck and Suzuki type reactions [42–49]. Based on the published results [42,50–53], a possible mechanism for bidentate-chelation catalytic systems such as pallada-and platinacycle-mediated for Suzuki–Miyaura and Mizoroki-Heck reactions are proposed in Scheme 2. We considered the metal oxidation states 0 and II in a cationic catalytic cycle. By employing the phosphine-based ligand and base as reducing agents, the active M(0) species were generated in an exothermic reaction leads to the formation of a π-coordinated complex as an intermediate (the mentioned reduction step is not a part of the catalytic cycle) [50,51].

The electrophilic attack of a metal center, Pd(0) or Pt(0), to the aryl chloride to form initially an arylated M(II) speciesis is the key step of the catalytic cycle leading to the π-coordinated intermediate. The resulting M(II) complex reacts with an olefin in the Heck reaction, or an arylboronic acid in the Suzuki reaction, respectively. Reductive elimination then produces the unique product for each reaction and regenerates the catalyst to begin the catalytic cycle again.

Using the optimized reaction conditions, we have tested two kinds of functionalized aryl chlorides bearing electron-donating to electron-withdrawing groups (Figuers 4 and 5). Based on the above results and literature, decreasing of electron density on the aryl

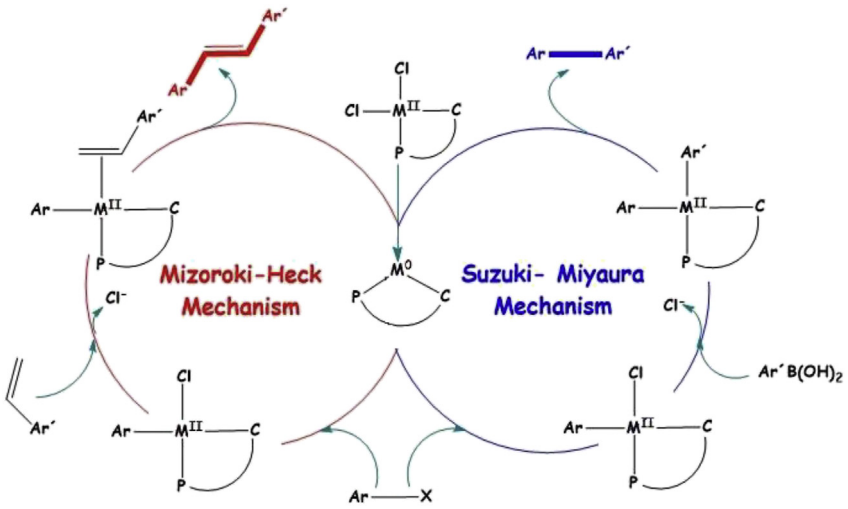

Scheme 2. Generic mechanisms for the Mizoroki–Heck and Suzuki– Miyaura reaction of the bidentate-chelation catalytic systems.

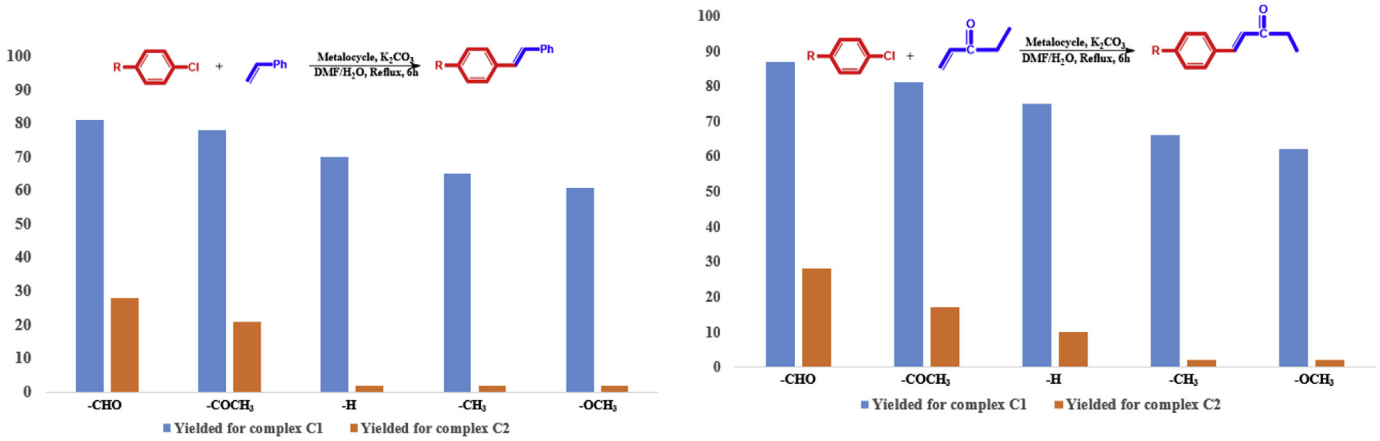

Fig. 4. Reaction conditions for Mizoroki-Heck coupling reaction: aryl chloride (0.5 mmol), olefin (0.75 mmol), K_2CO_3 (1 mmol), DMF/H_2O (2 ml), catalyst C1 (0.005 mmol), in air.

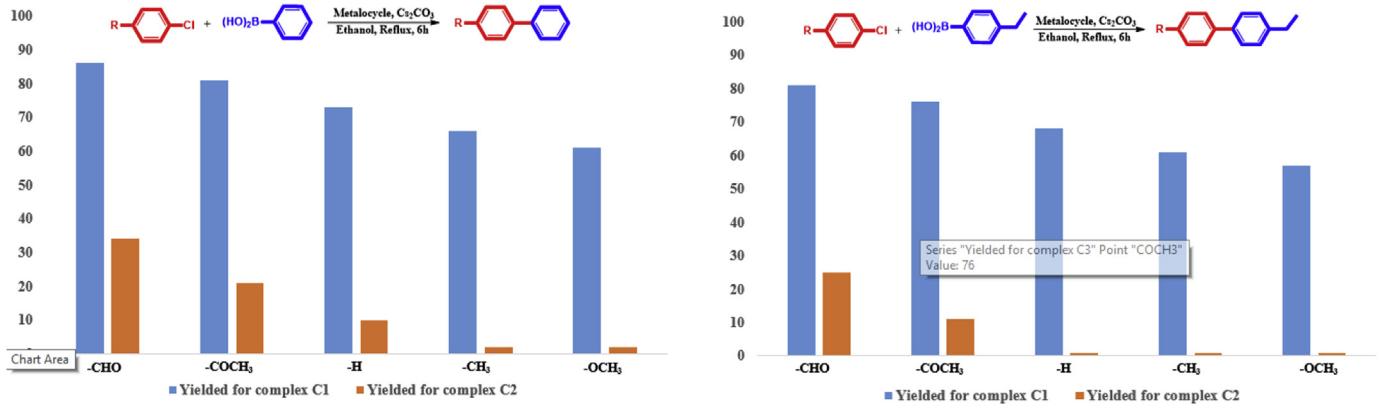

Fig. 5. Reaction conditions for Suzuki– Miyaura coupling reaction: aryl chloride (0.5 mmol), arylboronicacid (0.75 mmol), K_2CO_3 (1 mmol), DMF/H_2O (2 ml), catalyst C1 (0.005 mmol), in air.

chlorides increased the catalyst activity. That is, high yields are achieved when the relevant reagent reacts with aryl chlorides bearing the electron-withdrawing substituents –CHO and –$COCH_3$. Conversely, 4-chlorotoluene and 4-chloroanisol deactivated aryl chlorides gave lower yields indicating that the reaction was sensitive to the electron density on the aryl chlorides. The reaction of electronically neutral chlorobenzene with another reagent also produced a high yield of the product. This law applies to both Mizoroki-Heck and Suzuki–Miyaura coupling reactions. To extend the scope of our work, we investigated the coupling reaction of aryl

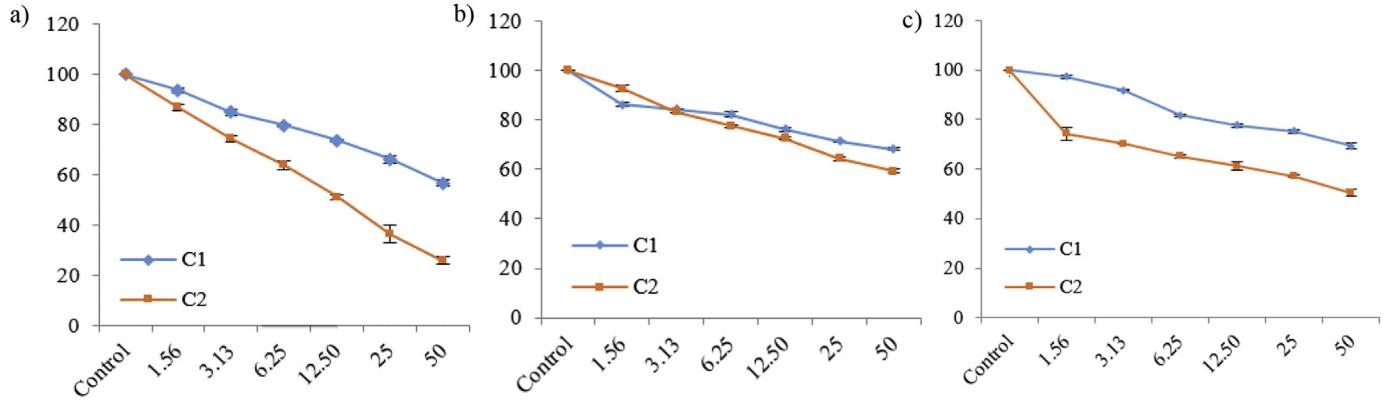

Fig. 6. Graphical representation of the anticancer activity of the synthesized compounds in the human different cancer cells: (a) AGS, (b) MCF-7, and (c) A-549 as obtained by the MTT assay. The experiment was performed in triplicate and expressed as mean ± SD.

chloride substrates with the more reactive reagent (ethyl acrylate for Heck and 4-ethylphenylbronic acid for another one). As expected, an electron-withdrawing substituent on the reagent has an increasing effect on the yield of the reaction.

The first important aspect of this study is the comparison of the catalytic properties of Pd(II) and Pt(II) complexes. Complex **C2,** in contrast to Complex **C1,** is expected to have less of an effect in the above coupling reactions. The results of this test can assist in determining the nature of the active species. As seen in the above mechanisms, we believe that reductive elimination of two chloride atoms of the complexes leads to the formation of a catalytically active low-coordinate M(0) species [54,55]. It is possible that similar reductive processes occur for the platinum complex; therefore, at this stage, we are not able to rule out the possibility of a Pt(II) cycle, although the use of strongly π-acidic ligands tends to mitigate of reductive elimination. When the activity of the complexes **C1** and **C2** in the couplings are compared, it can be seen that the order of activity is **C1**>**C2**. The fact that **C2** shows the lowest activity indicates the oxidative-addition step is being retarded compared to when **C1** is used. It would be expected that the rate of oxidative-addition for the palladium center in **C1** is higher, but the more difficult oxidative-addition at the platinum appears to be deleterious. So, the rate-determining step is probably the oxidative-addition step that makes Pd(II) complexes more active than Pt(II) complexs in the Mizoroki-Heck and Suzuki– Miyaura coupling reactions.

3.2.2. Cytotoxicity in vitro

The preliminary *in vitro* anti-proliferative efficiency of the novel tested compounds was studied by means of a colorimetric microculture assay (MTT assay) in the human gastric (AGS), breast (MCF-7), and lung (A549) cancer cells. Comparative cytotoxicity patterns of the Pd/Pt(II) compounds **C1** and **C2** for AGS, MCF-7, and A549 expressed as a percentage of cell viability are shown in Fig. 6. The half maximal inhibitory concentration (IC_{50} value) is a drug concentration required for inhibiting and killing 50% of the cells. IC_{50} values of the compounds, estimated from the dose-survival curves for the growth inhibition of three cell lines, are presented in Table 6. Generally, **C2** reveals a high anticancer activity compared to **C1**. The increase in potency for **C2** may be related to the nature of center metal, as both complexes are isostructural. Furthermore, AGS cells (Average of IC_{50} value; 61.19 μM) are more chemosensitive to the compounds studied in the current study than the MCF-7 and A449 cells, based on a comparison of IC_{50} amounts (Table 6).

Effects of the tested complexes on the viability of studied cancer cells, Fig. 6-a and Table 6, showed that the AGS cells were more susceptible to the compounds than the other two human adenocarcinoma cell lines. Based on our results, compound **C2** (IC_{50} values; 12.88 ± 1.09 μM) was strongly cytotoxic, much more than **C1** (IC_{50} values; 109.50 ± 36.22 μM). At lower doses, both complexes were tolerated by the AGS, and their anticancer activity, at 1.56 μM concentration, were >87%. In contrast to the results obtained by Budzisz et al. [56], our results showed that the Pt(II) complex had a higher antitumor impact towards the human gastric cell line than that of the Pd(II) complex.

Table 6
Comparison of cytotoxicity (IC50 values based on μM) of the synthesized compounds.

Compound	AGS	MCF-7	A549
C1	109.50 ± 36.22	149.58 ± 44.80	513.47 ± 122.77
C2	12.88 ± 1.09	124.69 ± 7.66	66.88 ± 24.42

*The experiment was performed in triplicate and expressed as mean ± SD. Values along each column with different superscripts are significantly different ($P < 0.05$).

Both compounds, **C1** and **C2**, when used against cancer cells, namely, the human breast adenocarcinoma (MCF-7), displayed IC_{50} values of 149.88 ± 44.88 and 124.69 ± 7.66 μM, respectively (Fig. 6-b and Table 6). At lower doses, the compound **C1** reveals higher cytotoxic action than **C2**. These findings were considerably higher than those reported by Ray et al. for the benchmark drug cisplatin with IC_{50} of 15 ± 2 μM, for this cancer cells [57]. Likewise, in the test on the human A549 cells at 1.56, 3.13, 6.25, 12.50, 25 and 50 μM concentrations of the studied compounds, **C2** exhibited the excellent cytotoxic properties with the half maximal inhibitory concentration (IC_{50}) of 66.88 ± 24.42 μM (Fig. 6-c and Table 6). Our findings also indicated that compound **C1** had a weak cytotoxic activity.

4. Conclusions

In summary, we report the synthesis and full characterization of new phosphorus ylide, pallada-and platinaphosphacycle complexes. On the basis of the spectroscopic data and X-ray analysis, the ligand Y exhibits P, C-coordination behavior to the metal centers and affords a five-membered ring. Furthermore, the catalytic activity of complexes towards the Mizoroki-Heck and Suzuki-Miyaura coupling reactions of various aryl chlorides were investigated. The results show that the coupling reactions with palladacycle as catalyst results in higher yields than the platinacycle, because of an easier oxidative-addition step. Additionally, the current study

presents evidence that the investigated compounds induce the anti-proliferative effect in the human gastric (AGS), breast (MCF-7), and lung (A549) cancer cells. Our data indicated that the compound **C2** was most cytotoxic than **C1** that it is due to Pt nature and ligand properties. It should be noted that although all *in vitro* experiments hold limitations with respects to possible *in vivo* efficiency, the results are very promising with regards to possible antineoplastic chemotherapy and form a very sound basis for future research.

Acknowledgements

Funding of our research from the Bu-Ali Sina University is gratefully acknowledged.

Appendix A. Supplementary data

Supplementary data to this article can be found online at https://doi.org/10.1016/j.jorganchem.2019.03.002.

References

[1] G. Ricci, et al., Well-defined transition metal complexes with phosphorus and nitrogen ligands for 1, 3-dienes polymerization, Coord. Chem. Rev. 254 (5–6) (2010) 661–676.
[2] S.J. Sabounchei, et al., Palladium (II) phosphine–ylide complexes as highly efficient pre-catalysts in additive-and amine-free Sonogashira coupling reactions performed under aerobic and low Pd loading conditions, Tetrahedron Lett. 54 (35) (2013) 4656–4660.
[3] S.J. Sabounchei, et al., Synthesis and structural characterization of dimeric phosphine ylide Cu (I) complexes: application in Suzuki cross-coupling reactions and biological evaluation as antibacterial agents, J. Organomet. Chem. 761 (2014) 111–119.
[4] S. Zhang, et al., Desulfitative Suzuki cross-couplings of arylsulfonyl chlorides and boronic acids catalyzed by a recyclable polymer-supported N-heterocyclic carbene-palladium complex catalyst, Synlett 2006 (12) (2006) 1891–1894.
[5] S.J. Sabounchei, et al., New chlorine bridged binuclear silver (I) complexes of bidentate phosphorus ylides: synthesis, spectroscopy, theoretical and antibacterial studies, Polyhedron 85 (2015) 652–664.
[6] J.A. Albanese, et al., Phosphorus ylides as hard donor ligands: synthesis and characterization of MCl4 (ylide-O)(THF)(M= Ti, Zr, Hf; ylide=(acetylmethylene) triphenylphosphorane,(benzoylmethylene) triphenylphosphorane). Molecular structure of trans-((acetylmethylene) triphenylphosphorane-O)(tetrahydrofuran) tetrachlorotitanium-(IV)-tetrahydrofuran, Inorg. Chem. 29 (12) (1990) 2209–2213.
[7] M.M. Ebrahim, H. Stoeckli-Evans, K. Panchanatheswaran, Reactivity of mercury (II) halides with the unsymmetrical phosphorus ylide Ph 2 PCH 2 CH 2 PPh 2 C (H) C (O) Ph: crystal structure of {HgI 2 [PPh 2 CH 2 CH 2 PPh 2 C (H) C (O) Ph]} n, Polyhedron 26 (14) (2007) 3491–3495.
[8] C. Shiju, et al., Synthesis, characterization, and biological evaluation of Schiff base–platinum (II) complexes, Spectrochim. Acta Mol. Biomol. Spectrosc. 145 (2015) 213–222.
[9] R. Chinchilla, C. Najera, Chemicals from alkynes with palladium catalysts, Chem. Rev. 114 (3) (2013) 1783–1826.
[10] N. Kuhl, et al., Formal SN-type reactions in rhodium (III)-catalyzed C-H bond activation, Adv. Synth. 356 (7) (2014) 1443–1460.
[11] K. Yamaguchi, N. Mizuno, Scope, kinetics, and mechanistic aspects of aerobic oxidations catalyzed by ruthenium supported on alumina, Chem. Eur. J. 9 (18) (2003) 4353–4361.
[12] P.D. Boyd, L.J. Wright, M.N. Zafar, Extending the range of neutral N-donor ligands available for metal catalysts: N-[1-Alkylpyridin-4 (1 H)-ylidene] amides in palladium-catalyzed cross-coupling reactions, Inorg. Chem. 50 (21) (2011) 10522–10524.
[13] F. Schroeter, T. Strassner, Understanding anionic “ligandless” palladium species in the Mizoroki–heck reaction, Inorg. Chem. 57 (9) (2018) 5159–5173.
[14] A. Biffis, et al., Pd metal catalysts for cross-couplings and related reactions in the 21st century: a critical review, Chem. Rev. 118 (4) (2018) 2249–2295.
[15] S.J. Sabounchei, et al., Pd (II) and Pt (II) complexes of α-keto stabilized sulfur ylide: synthesis, structural, theoretical and catalytic activity studies, J. Mol. Struct. 1135 (2017) 174–185.
[16] S.J. Sabounchei, et al., New Rh (III) complexes of 5-methyl-5-(pyridyl)-2, 4-imidazolidenedione: synthesis, X-ray structure, electrochemical study and catalytic behaviour for hydrogenation of ketones, Appl. Organomet. Chem. 31 (10) (2017) e3716.
[17] S.J. Sabounchei, et al., Mononuclear palladium (ii) and platinum (ii) complexes of P, C-donor ligands: synthesis, crystal structures, cytotoxicity, and mechanistic studies of a highly stereoselective Mizoroki–Heck reaction, J. Inorg. Chem. Front. 4 (12) (2017) 2107–2118.
[18] R.L. Siegel, K.D. Miller, A. Jemal, Cancer statistics, Canc. J. Clin. 67 (1) (2017) 7–30.
[19] Z. Almodares, et al., Rhodium, iridium, and ruthenium half-sandwich picolinamide complexes as anticancer agents, Inorg. Chem. 53 (2) (2014) 727–736.
[20] N. Farrell, Multi-platinum anti-cancer agents. Substitution-inert compounds for tumor selectivity and new targets, Chem. Soc. Rev. 44 (24) (2015) 8773–8785.
[21] S. Nussbaumer, et al., Analysis of anticancer drugs: a review, Talanta 85 (5) (2011) 2265–2289.
[22] B. Rosenberg, L. Van Camp, T. Krigas, Inhibition of cell division in Escherichia coli by electrolysis products from a platinum electrode, Nature 205 (4972) (1965) 698–699.
[23] M. Xie, et al., Unusual dimeric chemical structure for a carboplatin analogue as a potential anticancer complex, Inorg. Chem. 49 (13) (2010) 5792–5794.
[24] N.J. Wheate, et al., The status of platinum anticancer drugs in the clinic and in clinical trials, Dalton Trans. 39 (35) (2010) 8113–8127.
[25] G.M. Cragg, P.G. Grothaus, D.J. Newman, Impact of natural products on developing new anti-cancer agents, Chem. Rev. 109 (7) (2009) 3012–3043.
[26] F. Samari, et al., Affinity of two novel five-coordinated anticancer Pt (II) complexes to human and bovine serum albumins: a spectroscopic approach, Inorg. Chem. 51 (6) (2012) 3454–3464.
[27] S.J. Sabounchei, et al., Synthesis, characterization and structural studies of new palladium (II) complexes including non-symmetric phosphorus ylides, Inorg. Chim. Acta 363 (14) (2010) 3973–3980.
[28] D. Drew, J. Doyle, A.G. Shaver, Cyclic diolefin complexes of platinum and palladium, Inorg. Synth. 13 (1972) 47–55.
[29] Rigaku Oxford Diffraction, CrysAlisPro Software system, version 1.171.39.46, Rigaku Corporation, Oxford, UK, 2018.
[30] Dolomanov, et al., OLEX2: a complete structure solution, refinement and analysis program, J. Appl. Cryst. 42 (2009) 339–341.
[31] G.M. Sheldrick, SHELXT - Integrated space-group and crystal-structure determination, Acta Cryst. A71 (1) (2015) 3–8.
[32] G.M. Sheldrick, Crystal structure refinement with SHELXL, Acta Cryst. C71 (1) (2015) 3–8.
[33] Y. Garcia, et al., Theoretical bond dissociation energies of halo-heterocycles: trends and relationships to regioselectivity in palladium-catalyzed cross-coupling reactions, J. Am. Chem. Soc. 131 (18) (2009) 6632–6639.
[34] A. Fürstner, A. Leitner, General and user-friendly method for Suzuki reactions with aryl chlorides, Synlett 2001 (02) (2001) 0290–0292.
[35] C. Lau, et al., Cytotoxic activities of Coriolus versicolor (Yunzhi) extract on human leukemia and lymphoma cells by induction of apoptosis, Life Sci. 75 (7) (2004) 797–808.
[36] M. Sylvestre, et al., Chemical composition and anticancer activity of leaf essential oil of Myrica gale L, Phytomedicine 12 (4) (2005) 299–304.
[37] M. Kalyanasundari, et al., Reactions of benzoylmethylenetriphenylphosphorane with mercury (II) halides: spectral and structural characterization of [(C6H5) 3PCHCOC6H5· HgCl2] 2· 2CH3OH and [(C6H5) 3PCHCOC6H5· HgI2] 2, J. Organomet. Chem. 491 (1–2) (1995) 103–109.
[38] S.J. Sabounchei, A. Hashemi, Ylides: Synthesis, Reactions and Applications, vol 27, Nova Science Publishers, Inc, 2015.
[39] S.J. Sabounchei, et al., New Pd/Pt-[60] fullerene complexes of phosphorus ylides as anticancer agents: cytotoxic investigation and DFT calculations, J. Organomet. Chem. 860 (2018) 49–58.
[40] R. Uson, et al., Cationic palladium (II) complexes involving unprecedented O-coordination of acetylmethylenetriphenylphosphorane, J. Organomet. Chem. 290 (1) (1985) 125–131.
[41] G. Facchin, et al., Synthesis and characterization of palladium (II)-η 3-allyl–ylide complexes. X-Ray crystal structure of [PdCl (η 3-2-MeC 3 H 4) {Ph 3 PC (H) COMe}], Dalton Trans. (6) (1987) 1381–1387.
[42] Z.L. Niemeyer, et al., Parameterization of phosphine ligands reveals mechanistic pathways and predicts reaction outcomes, Nat. Chem. 8 (6) (2016) 610.
[43] C. Amatore, A. Jutand, Anionic Pd (0) and Pd (II) intermediates in palladium-catalyzed Heck and cross-coupling reactions, Acc. Chem. Res. 33 (5) (2000) 314–321.
[44] J. Lindh, et al., Efficient palladium (II) catalysis under air. Base-free oxidative heck reactions at room temperature or with microwave heating, J. Org. Chem. 72 (21) (2007) 7957–7962.
[45] J.P. Knowles, A. Whiting, The Heck–Mizoroki cross-coupling reaction: a mechanistic perspective, Org. Biomol. Chem. 5 (1) (2007) 31–44.
[46] A. Suzuki, Carbon–carbon bonding made easy, Chem. Commun. (38) (2005) 4759–4763.
[47] A. Suzuki, Cross-coupling reactions of organoboranes: an easy way to construct C-C bonds (nobel lecture), Angew. Chem. Int. Ed. 50 (30) (2011) 6722–6737.
[48] A.K. Diallo, et al., “Homeopathic” catalytic activity and atom-leaching mechanism in Miyaura–suzuki reactions under ambient conditions with precise Dendrimer-stabilized Pd nanoparticles, ngewandte Chemie 119 (45) (2007) 8798–8802.
[49] Y.M. Kim, S. Yu, Palladium (0)-catalyzed amination, Stille coupling, and Suzuki coupling of electron-deficient aryl fluorides, J. Am. Chem. Soc. 125 (7) (2003) 1696–1697.
[50] T.W. Lyons, M.S. Sanford, Palladium-catalyzed ligand-directed C– H functionalization reactions, Chem. Rev. 110 (2) (2010) 1147–1169.
[51] L. Ackermann, R. Vicente, A.R. Kapdi, Transition-metal-catalyzed direct arylation of (hetero) arenes by C-H bond cleavage, Angew. Chem. Int. Ed. 48 (52) (2009) 9792–9826.

[52] P.L. Arrechea, S.L. Buchwald, Biaryl phosphine based Pd (II) amido complexes: the effect of ligand structure on reductive elimination, J. Am. Chem. Soc. 138 (38) (2016) 12486–12493.
[53] C. Amatore, A. Jutand, M.A. M'Barki, Evidence of the formation of zerovalent palladium from Pd (OAc) 2 and triphenylphosphine, Organometallics 11 (9) (1992) 3009–3013.
[54] R.B. Bedford, S.L. Hazelwood, D.A. Albisson, Platinum catalysts for Suzuki biaryl coupling reactions, Organometallics 21 (13) (2002) 2599–2600.
[55] C. Mateo, et al., Intramolecular transmetalation of arylpalladium (II) and arylplatinum (II) complexes with silanes and stannanes, Organometallics 17 (17) (1998) 3661–3669.
[56] E. Budzisz, et al., Synthesis, crystal structure and biological characterization of a novel palladium (II) complex with a coumarin-derived ligand, Eur. J. Inorg. Chem. 2004 (22) (2004) 4412–4419.
[57] S. Ray, et al., Anticancer and antimicrobial metallopharmaceutical agents based on palladium, gold, and silver N-heterocyclic carbene complexes, J. Am. Chem. Soc. 129 (48) (2007) 15042–15053.